Aero-Hydrodynamic Interactions for Wind Powered Ships: Retrofit of a High-Speed Mega RoRo Vessel

Nico van der Kolk, AlbatrosDigital, Rotterdam/The Netherlands, nico@albatros.digital
Theo Tardif, Computed Wing Sail, Paris/France, theo.tardif@computedwingsail.com
Francesco Stella, Computed Wing Sail, Paris/France, francesco.stella@computedwingsail.com
Gunnar Jacobi, Delft University of Technology, Delft/The Netherlands, g.jacobi@tudelft.nl

Abstract

This study evaluates the retrofit of a high-speed RoRo vessel with rigid wingsail wind propulsion, focusing on aero-hydrodynamic interactions and real-world performance. A validated lifting line model, enhanced with CFD-derived ship-sail interaction effects, is coupled with a dynamic vessel simulation environment. Using operational data from HUMBRIA SEAWAYS, we simulate fuel savings and vessel response across realistic voyages. Results show median fuel savings of 16% at 18 kn, with effective course-keeping and no major operational penalties. The findings support the viability of wind propulsion retrofits for fast RoRo ships operating on consistent, wind-exposed trade routes.

Nomenclature

ΔR_WPS	Change in resistance due to WPS (kg m s^{-2})
AWA	Apparent wind angle - ship frame (°)
AWS	Apparent wind speed - ship frame (m s^{-1})
CII	Carbon Intensity Indicator (gCO_2 $GT^{-1}{\cdot}nm^{-1}$)
F_WPS	Aerodynamic thrust (kg m s^{-2})
R_T	Ship resistance including wind and wave resistance (kg m s^{-2})
Span	Height of wind propulsion system (m)
TB	Thrust benefit (%)
Vs	Ship speed (kn)

1. Introduction

The maritime industry is under intense pressure to rapidly decarbonize. Owners and operators are obliged to improve the efficiency of their ships to comply with emissions regulations. Wind propulsion systems (WPS) stand apart among the near-term retrofit options. Simply put, wind provides carbon-free propulsion. Ships fitted with wind propulsion technologies can maintain speed while reducing fuel consumption. Especially along windy routes, the impact on vessel environmental efficiency metrics such as Carbon Intensity Indicator (CII) can be profound.

Wind propulsion systems (WPS) are increasingly adopted, particularly in deep-sea bulker and tanker fleets which benefit from generally low ship speeds and good available deck space for integration. For RoRo vessels operating at high speeds (Vs greater than ~18 kn), the vessels own speed and apparent wind will detrimentally shift apparent wind angle (AWA) forwards, resulting in predominantly upwind sailing conditions where aerodynamic and sailing efficiency are essential to realise significant fuel savings. RoRo types do offer clear deck space for wind propulsion integration, as well as regular sailing tracks and schedules that allow straightforward techno-economic projections about the benefit of a wind propulsion retrofit or newbuilding option.

Several RoRo vessels have been retrofitted with wind propulsion systems, chief among which is Sea-Cargo's SC CONNECTOR, Fig.1. SC CONECTOR is 154 m long with capacity of approximately 1,775 lane meters and a service speed of around 11 kn. It was retrofitted with two 35 m tiltable Norsepower rotor sails in 2021. According to Sea-Cargo and Norsepower, the vessel is able to operate on wind power alone in favourable conditions, with reported annual yields of approximately 25% along North Sea routes. Utilisation of this ship has changed to maximise the wind-powered contribution to

propulsion, where the shortest-distance route is replaced by active voyage optimisation considering each update to the weather forecast. Furthermore, vessel stability in seaway is much improved due to aerodynamic added-mass and damping effect of the WPS.



Fig.1: Sea-Cargo's SC CONNECTOR fitted with wind propulsion systems. Source: dnv.com

Captain Artur Sylwestrzak of the SC CONNECTOR, highlights both performance and crew benefits. "The vessel behaves much better," he explains, referring to the improved roll damping and overall seakeeping. He describes the ship's motion as "more stable," adding that this directly translates to increased comfort and safety on board. Captain Sylwestrzak also appreciates the operational advantages, stating, "We are now using wind as a free and unlimited source of energy," and emphasizes the importance of his crew's enthusiasm: "Once they understood how it works, they became proud to be part of something innovative," *DNV (2023)*.



Fig.2: Newbuilding RoRo's with WPS announced by Louis Dreyfus Armateurs (top-left), source: lda.fr, Willenius Wilhemson (bottom-left) source: walleniuswilhelmsen.com, Neoline (top-right) source: neoline.fr, and Stena Line (bottom-right) source: stenaline.com

This encouraging experience suggests that significant wind yields might be within reach for most of the RoRo fleet, sailing in the Northern Sea and elsewhere. Nevertheless, the ability of WPS to deliver high thrust even at significantly higher ships speeds is a crucial element of the business case for wind propulsion. In this respect, rigid wingsails, such as CWS Airfin350, have a significant edge of other WPS, due to their naturally high sailing efficiency. This study builds upon previous techno-economic analyses and hydrodynamic research to incorporate an advanced modelling for wingsail aero-dynamics, including superstructure-disturbed windage and optimal sail control considering aero-dynamic interactions to provide a detailed exploration of integrated aerodynamic and hydrodynamic solutions specifically tailored to the needs of a high-speed RoRo retrofit case, sailing at 17-19 kn.

2. Background

European carriers have initiated significant investments in fleet renewal and retrofitting programs. For example, CLdN introduced LNG dual-fuel vessels specifically designed for European short-sea routes, while DFDS deployed new Jinling-built RoRo ferries optimized for efficiency within European waters. Deep-sea operators based in Europe, such as Wallenius Wilhelmsen and Grimaldi Group, have similarly expanded capacities with next-generation vessels to meet high vehicle transport demands.



Fig.3: HUMBRIA SEAWAYS is a modern mega-RoRo cargo ferry built in 2020 operating on the Gothenburg (Sweden) – Ghent (Belgium) route. WPS retrofit concept shown.

DFDS is one of Europe's leading short-sea RoRo operators, running a pan-European network of freight ferry routes spanning the North Sea, Baltic Sea, English Channel, and Mediterranean. The company places a strong emphasis on decarbonisation, putting sustainability first and investing in innovative technologies to reduce its environmental footprint. DFDS were willing to contribute technical specifications and operational data to this case study including vessel particulars, voyage reports, and one year of AIS tracks.

HUMBRIA SEAWAYS operates a fixed route between Gothenburg and Ghent. The Gothenburg–Ghent corridor presents an operationally relevant test case for evaluating wind-assisted propulsion performance. Spanning approximately 550 nm across the North Sea, the route is characterized by frequent exposure to westerly and south-westerly winds, particularly during the autumn and winter months. Average wind speeds along the corridor range between 6–10 m/s, with persistent moderate sea states, making it suitable for steady-state wind-assist operation. The route's duration of approximately 32 h at a typical service speed of 17–19 kn provides sufficient exposure time for aero-dynamic thrust to contribute measurably to propulsion. Additionally, the route avoids narrow

passages or air-draft constraints. These conditions, combined with consistent biweekly scheduling and a high-capacity RoRo hull form, position the HUMBRIA SEAWAYS as an ideal candidate for evaluating real-world integration of aerodynamic and hydrodynamic design innovations.

Table I: Main particulars of DFDS ship: HUMBRIA SEAWAYS

Build Year	2020
Length	237.40 m
Breadth	33.00 m
Draft	6.65 m
Dead Weight (Scantling)	17183 tdw
Gross Tonnage	60465 t
Lane Length	6700 m
Capacity (trailers)	450
Propulsion Power	23.6 MW

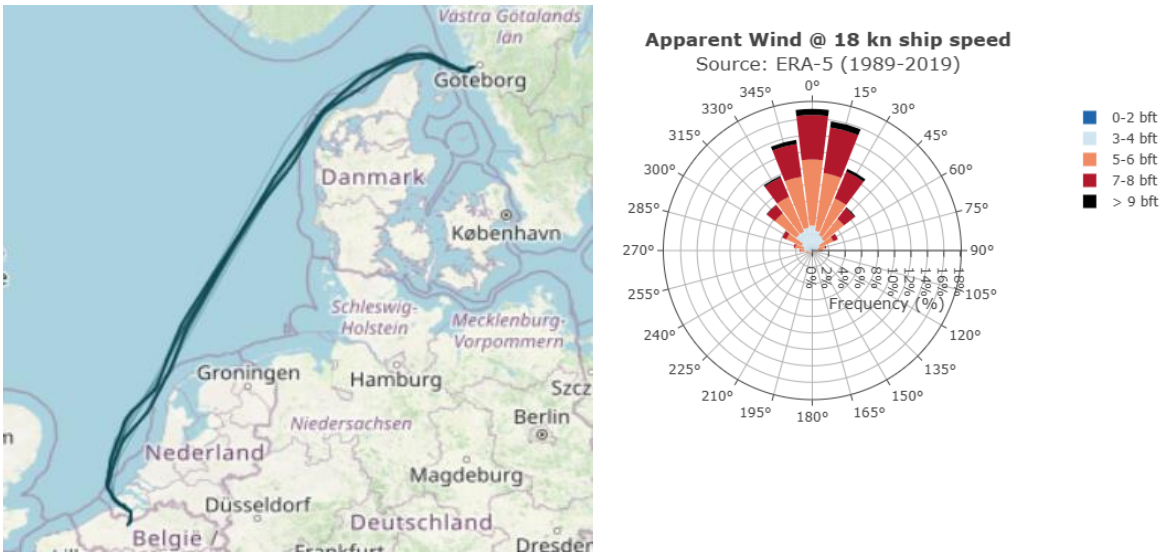


Fig.4: AIS track of HUMBRIA SEAWAYS route between Gothenburg and Ghent during 2024 (left), wind-rose plot showing distribution of apparent wind on round-trip voyage (right) source: MARIN Blue Route.

An overview of HUMBRIA SEAWAYS operational profile and associated wind conditions is presented in Fig.4. AIS data for q4 2024 data represents 45 voyages, where due to data gaps 28 tracks are retained for analysis. A 30-year representation of apparent wind statistics is shown in top-right, including 18 kn ship speed. The impact of vessel speed on apparent wind condition is clear, with normal transit speed at sea of 17-19 kn. The wind propulsion system and integration with the ship must have superior upwind capabilities.

3. Methodology and Results

Analysis in this paper presents aerodynamic modelling from CWS, and ship modelling and operational analysis from AlbatrosDigital. The following paragraphs outline methodology and results of individual efforts. Coupling between simulation tools followed an iterative approach, where AlbatrosDigital provided initial and revised hydrodynamic cost functions, representing the sailing-induced drag associated with drift force and yawing moment (rudder working). These cost functions were used by CWS to refine the Aerodynamic trim of Airfin350 wingsails in upwind conditions. Finally, the aerodynamic forces and moments of the wingsail arrangement are imposed on the AlbatrosDigital ship model with a 6dof tabular exchange format.

3.1. Aerodynamic Modelling

Precise modelling of aerodynamic interactions is crucial to accurately predict performance of multi-sail Wind Propulsion System (WPS) configurations, such as CWS Airfin350 wingsails. We began with a fundamental approach to single sail modelling before addressing the complexities of sail-sail and ship-sail interactions.

3.1.1. Aerodynamic Single Sail Modelling

The first layer of the aerodynamic model uses Prandtl's Lifting Line Model (LLM) to predict a reliable performance baseline for a single Airfin350 wingsail. The LLM is a well-established aerodynamic tool that calculates the spanwise lift distribution, considering the influence of trailing vortices. For the Airfin350, LLM was extensively validated against experimental data obtained from wind tunnel tests run at a Reynolds number (Re) of 10^6, on an isolated Airfin350 wingsail. Measurements took place in the S10 wind tunnel of the Institute Aerotechnique (IAT-CNAM). The LLM predictions showed a satisfactory agreement with the experimental results for the single wingsail, confirming its suitability as a basis for further, more complex modelling. This validated single sail model served as the foundation for developing our multi-sail interaction models and sail-ship hull and superstructure interaction models.

3.1.2. Aerodynamic Sail-Sail Interaction Modelling

Interactions between multiple wingsails are modelled by adding a horseshoe vortex system similar to CORR-SILL, *Malmek et al. (2020)*, to LLM. The algorithm iteratively solves the LLM for each wingsail, considering the induced velocities from other units, until convergence. CORR-SILL has known limitations, particularly in neglecting viscous effects and other terms of the Navier-Stokes equations. This is why several corrections were applied to the CORR-SILL model:

1. Pressure Gradient Correction: Following *Malmek et al. (2024)*, a boundary layer correction accounts for changes in local pressure on interacting wingsails, modifying the 2D lift curve used in the LLM and improving stall prediction.
2. Wingsail Viscous Wake: a semi-empirical correction, based on *Bordogna et al. (2016)*, models the viscous wake downstream of each wingsail, accounting for the velocity deficit related to drag.
3. Swirl Velocity Correction Inside the Vortex Core: To better represent tip vortices, which significantly influence interactions, we used the work by *Bhagwat and Leishman (2002)* to adjust swirl velocities within the vortex core, preventing local stall artifacts and improving interaction predictions when wingsails are aligned with the wind.
4. Streamwise Velocity Deficit Inside the Vortex Core: A streamwise velocity deficit was introduced within the vortex core, similar to the viscous wake. This also serves to represent the wake of the pedestal on which the wingsail is mounted, which was experimentally observed to have a notable impact on downstream wingsails.

The aerodynamic sails-sail interaction model was then validated and fine-tuned using experimental data from wind tunnel tests. Experiments were run on two large scale models attaining Re = 10^6, placed in several different layouts, Experimental results and model validations are extensively described in *Tardif et al. (2024)*.

3.1.3. Aerodynamic Ship-Sail Interaction Modelling

A ship-sail interaction model was added to account for the influence of the ship's superstructure on the airflow around the wingsails. Firstly, the perturbed flow field caused by the ship's hull and superstructure was computed with RANS simulation, for a set of wind speeds and directions. These perturbed fields were then used as input for the LLM calculations in the interaction model. This approach is supported by existing literature, such as the work by *Garenaux and Schot (2021)*, which

suggests that wind twist and the effect of the operating settings of the wind propulsor can be neglected in ship-sail interaction analyses. This simplifies the modeling process, allowing us to reduce the number of CFD configurations.

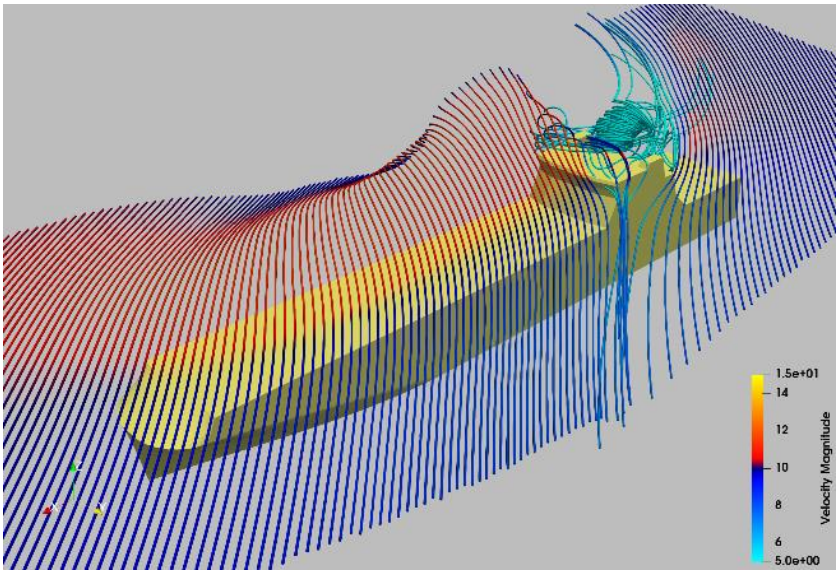


Fig.5a: Streamlines of the CFD flow field around the ship without wingsails

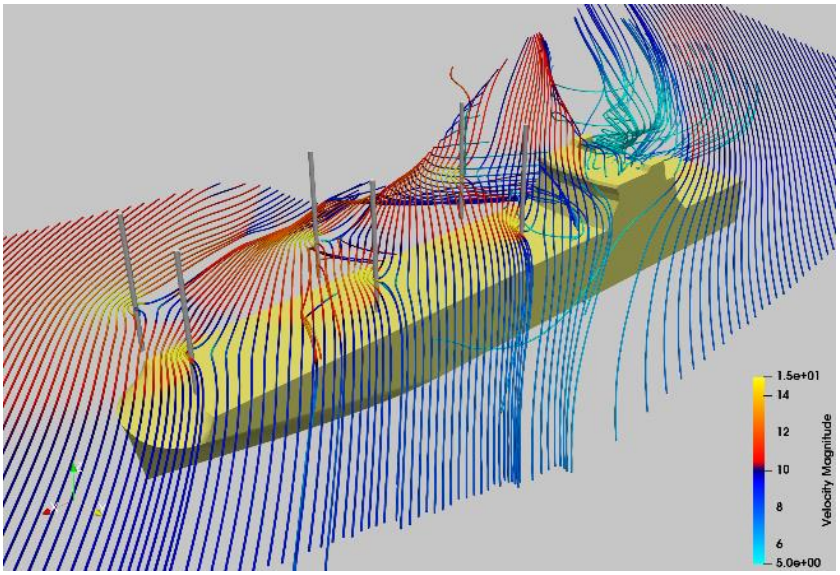


Fig.5b: Streamlines of the CFD flow field around the ship added to the induced velocities computed by the interaction model

It must be acknowledged that this methodology comes with inherent limitations. The perturbation field extracted from CFD corresponds to a steady-state mean flow and is then simply added to the induced velocities computed by the aerodynamic model. This linear superposition neglects potentially significant flow features such as local pressure gradients and turbulence-related phenomena, which could influence the aerodynamic response of the wingsails in a real operating environment.

Nonetheless, this method provides a first-order approximation of the aerodynamic interaction between ship and sails, enabling a more realistic evaluation of wingsail performance while maintaining reasonable computational cost. The superposition of the sail-sail and ship-sail interaction model is illustrated on Fig.5b. Our results confirm conclusions found in the literature: the apparent wind angle is shifted to the beam at low and high wind angles, while the apparent wind speed tends to decrease for beam winds.

3.1.4. CFD Setup Overview

The CFD simulations of the ship are run using OpenFOAM (version 22.12 by OpenCFD, on Ubuntu 22.04 LTS) on the CWS computing cluster. The simulations use the SIMPLE algorithm in combination with the k-ω SST turbulence model. The computational domain is a cylindrical volume with a diameter of 900 m and a height of 130 m. It features a single inlet and a one outlet, with two symmetry planes enclosing the remaining boundaries. A simplified representation of part of the ship above the water is placed at the bottom centre of the domain. The mesh consists of approximately 19 million cells.

Considering the symmetry of the ship, simulations were run on only one side of the vessel. The range of apparent wind angle (AWA) was sampled at every 15°, between 0° and 180°, for a reference apparent wind speed of 10 m/s. The aerodynamic model then applies a 4D linear interpolation across three spatial directions and the AWA to reconstruct the locally disturbed flow along the span of the wingsails. The velocities are scaled by AWS, which assumes flow similarity and neglects potential Reynolds number sensitivity.

3.2. Aerodynamic Results

In this section, we present the aerodynamic results obtained from our models and simulations. We will first examine the airflow perturbations caused by the presence of the ship and then analyze the aerodynamic performance of the complete rig, considering interactions between the sails and the ship.

3.2.1. Ship aerodynamic perturbations

Raw CFD results were analysed to assess whether the main flow trends align with observations from previous studies. Three representative AWA conditions are presented here: 45°, 90°, and 135°.

Fig.6a shows a deviation of the flow above the forward deck, where the wingsails are intended to be installed. This deviation locally shifts the apparent wind angle (AWA) towards a more favourable downwind direction. A slight increase in AWS is also observed in this region. Both effects are expected to improve the aerodynamic performance of the rig by increasing thrust while reducing the side force, compared to a scenario without ship-induced perturbations.

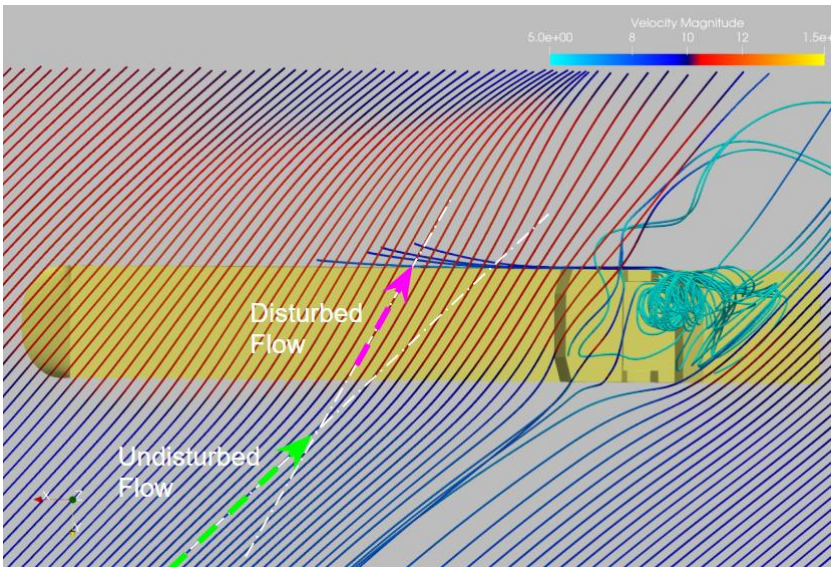


Fig.6a: Top view of streamlines of perturbated flow at AWA = 45° at Z=40 m

Fig.6b provides insight into the vertical distribution of the flow at beam winds (AWA = 90°). While an increase in wind speed is still noticeable above deck, a large recirculating bubble due to

flow separation is clearly visible. Within this region, the flow is highly turbulent and characterized by low velocities, which would significantly reduce the aerodynamic performance of the wingsails operating in this area. As a result, this phenomenon would likely mitigate the beneficial effects of the ship-induced flow acceleration on the wingsails.

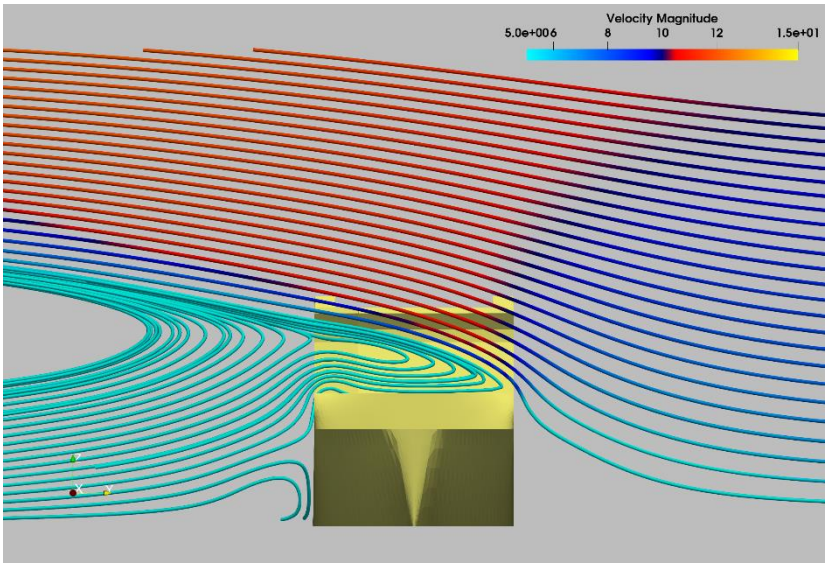


Fig.6b: Front view of streamlines of perturbated flow sampled at midship at AWA = 90° at Z=40 m

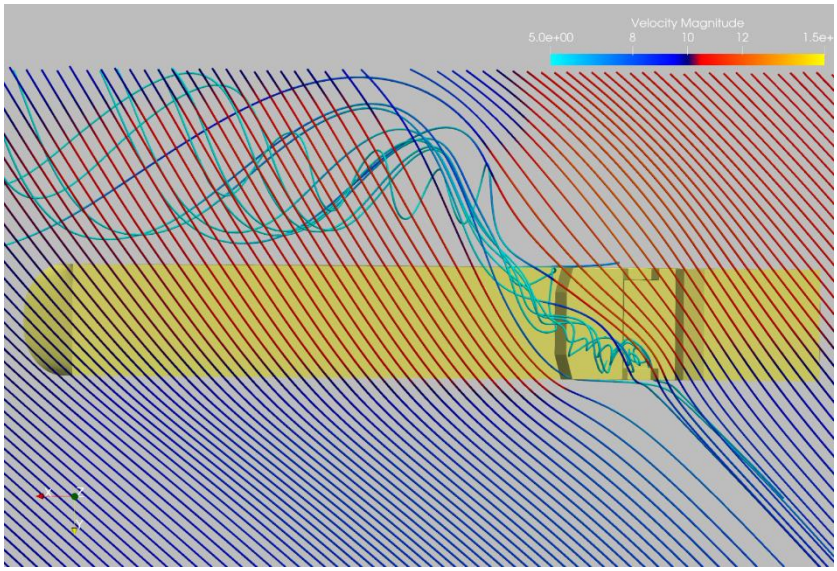


Fig.6c: Top view of streamlines of the perturbated flow at AWA = 135°. Z=40 m

Finally, Fig.6c shows flow characteristics at AWA of 135°. In this case, both flow deviation and velocity increase are less pronounced than at lower AWA, such as 45°. Additionally, the wake generated by the ship's superstructure would, in certain conditions, directly interact with the wingsails, potentially degrading their aerodynamic performance.

3.2.2. Full rig aerodynamic analysis

Several simulations were run to assess the overall aerodynamic performance of the wingsail rig, and to progressively account for the different interaction effects impacting the flow.

Three levels of modelling were considered. The first one included only the aerodynamic interaction between sails, without considering flow perturbations generated by the ship. In a second step, the

CFD-derived perturbed velocity field was introduced to capture the effect of the ship-sail interaction, considering the distortion of the flow induced by the hull and superstructure. Finally, a hydrodynamic penalty was added to the sail control optimiser, to represent the additional drag generated by the hull and appendages when compensating for the aerodynamic drift force.

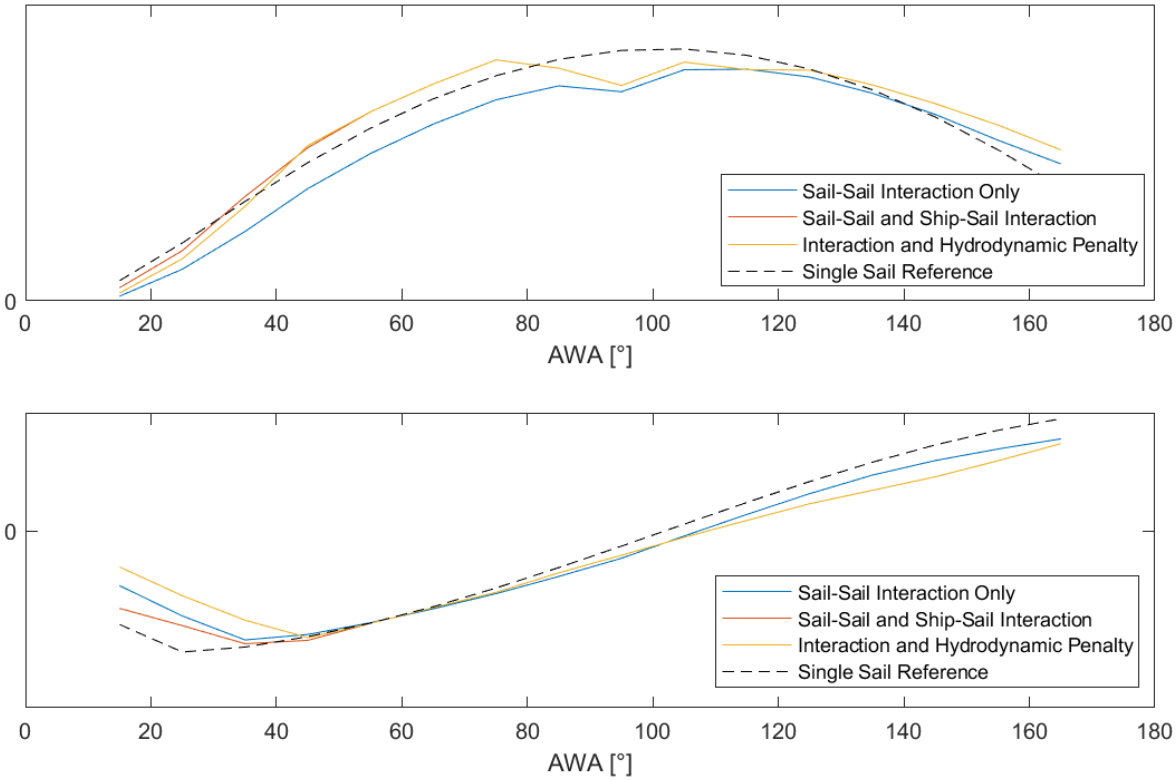


Fig.7: Evolution of thrust force (top) and drift force (bottom) as function of apparent wind angle

Fig.7 presents the total aerodynamic forces obtained for all tested configurations, including these different levels of modelling. The results are also compared to a single-sail reference case, which serves as a baseline for assessing the influence of sail-sail and ship-sail interactions.

Under upwind conditions, the interaction between sails significantly reduces the apparent aspect ratio of the rig, resulting in a sizable reduction in thrust. At beam wind conditions (AWA ≈ 90°), the wake shed by the sails on one board of the ship directly impacts the sails located downstream on the opposite board. This leads to a distinct thrust loss around 90° AWA. However, at higher AWAs, the aerodynamic interaction between sails becomes favourable, resulting in a thrust increase compared to the single-sail configuration.

The addition of ship perturbations has a mixed effect on sail performance, depending on AWA. Their influence is most significant at bow and to a lesser extent stern quartering AWA. The CFD velocity fields reveal both a favourable flow deviation and an increase in wind speed in the region where the wingsails are located. This has directly increases the thrust generated by the rig, as confirmed by the interaction model results. At beam wind conditions, the perturbations induced by the ship appear to have a limited effect on the overall aerodynamic forces. The local increase in wind speed above the deck tends to compensate for the performance losses generated at lower heights by the large recirculating bubble induced by flow separation.

Finally, the application of the hydrodynamic penalty mainly affects low AWA conditions (below 40°), where the drift force generated by the rig is the highest. The optimiser tends to reduce the angle of attack of the sails to limit the drift force, resulting in a slight decrease in thrust. Superior aerodynamic efficiency of the CWS Airfin350 profile, means that a significant reduction in drift force

can be achieved with only a moderate impact on thrust. At higher AWAs, where the drift force is naturally lower, the penalty has a negligible effect on the results.

3.3. Operational Performance Simulations

3.3.1. ALBATROSDIGITAL Software

The AlbatrosDigital software is a cloud-based modelling suite of naval architecture and marine engineering tools. At its core, the AlbatrosDigital software uses a constrained-optimization solver that computes a ship's response to maintain a steady course under given environmental conditions, such as ship speed, wind condition and wave condition. An adjustable level of simulation physics is available to match the modelling purpose, or available ship information. The Albatros software is highly customizable, allowing users to easily include their own specific models and requirements. The AlbatrosDigital software provides an assessment of the wind propulsion arrangements on the DFDS vessel HUMBRIA SEAWAYS

The model is deployed on a modern web-based infrastructure, featuring a cloud-native modelling engine that includes rapidly scalable computing resources. This architecture allows for efficient processing of large datasets and complex simulations. The model's flexibility extends to its integration with client data and third-party services, offering bespoke preconditioners and plug-ins that can be customized to meet specific needs. Users can interact with the tool using Jupyter Notebooks for input and output, an API endpoint integration, or a customized interface.

AlbatrosDigital Virtual Voyage makes the link to operational profiles, using HUMBRIA SEAWAYS AIS track provided by DFDS and metocean data to replicate voyages. The ship model comprises a full factorial combination of vessel drafts, vessel speeds, wind conditions, and wave conditions. For this analysis, the resulting fuel table consisting of 167,832 entries describing the vessel response. Along the waypoints of each AIS track, corresponding metocean data is matched to the relevant entry in the fuel table.

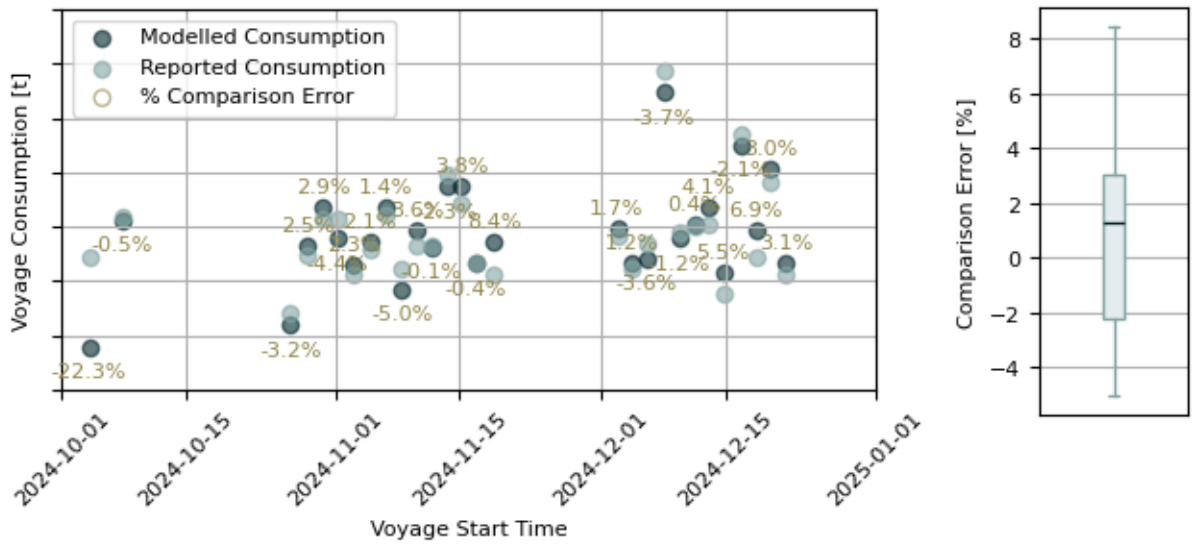


Fig.8: Modelling accuracy for AlbatrosDigital baseline model, comparing modelled voyage consumption with reported consumption in 28 DFDS voyage reports during q4 2024

A baseline digital ship model is first compared with consumption data in DFDS voyage reports to validate the composition of the model. Normal consumption is 60-110 t according to the weather encountered on the voyage. Over 28 complete AIS tracks during q4 2024, an MAPE level of 3.63% was reached, see Fig.8.

3.3.2. Concept design for WPS retrofit

A six-wingsail arrangement (three in-line along each deck edge) is proposed as maximal option for wind propulsion retrofit. We consider alternate configurations with three or four wingsails arranged along the centerline that may result in more efficient sailing performance. The leeward systems in the six-wingsail arrangement shown above suffer to a certain extent from the wake of the upwind systems. On the other hand, a six-wingsail arrangement along deck-edge facilitates integration with trailer operations on the upper deck.

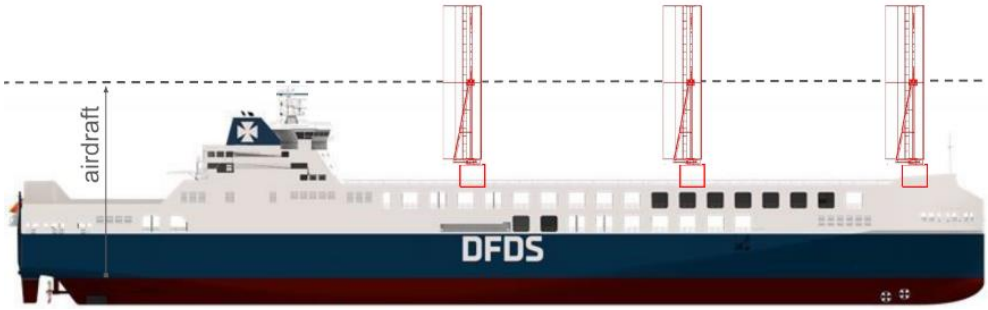


Fig.9a: Arrangement of six or three wingsails configuration on the ship deck

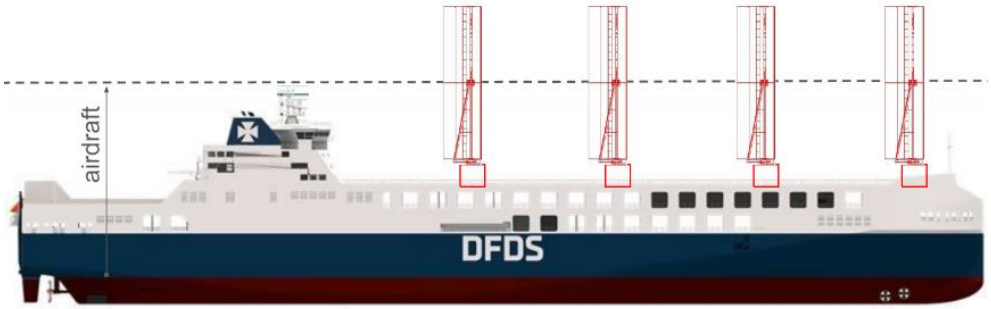


Fig.9b: Arrangement of four wingsails configuration on the ship deck

3.3.2. Thrust Benefit as Wind-assist design metric

The thrust benefit (TB) is a convenient performance metric for wind-hybrid vessels, defined as:

$$TB = \frac{F_{WPS}}{R_T + \Delta R_{WPS}}$$

Hence the thrust benefit is the ratio of the aerodynamic driving force produced by the wind propulsion system and the total the total resistance of the ship, including any increase due to the ‘sailing condition’. TB, often expressed as a percentage, represents the balance between wind propulsion and the main engine propulsion, and is therefore an approximation for the expected fuel savings. This level of analysis does not consider changes in the propulsion efficiency of the main mover (main engines and propellers).

Sailing performance metrics such as TB are typically presented in polar plots as in Fig.10, in which the vessel performance is given for a range of true wind speed (TWS) and for all wind angles (TWA). The angle is defined in the ship reference frame, relative to the ship heading: the ship is sailing directly into the wind at TWA = 0º (resulting in negative TB due to the added air drag of the wing-sails), and with the wind astern for TWA=180º. Observe the iso-line = 0 which defines the extents of the "no-go zone". At AWA = 115°, TB approaches 100% and some wingsail configurations supply enough thrust to propel the ship. The typical transit speeds for HUMBRIA SEAWAYS mean that wind angles are concentrated to "close-hauled" region where wind angles less than 60° are relevant.

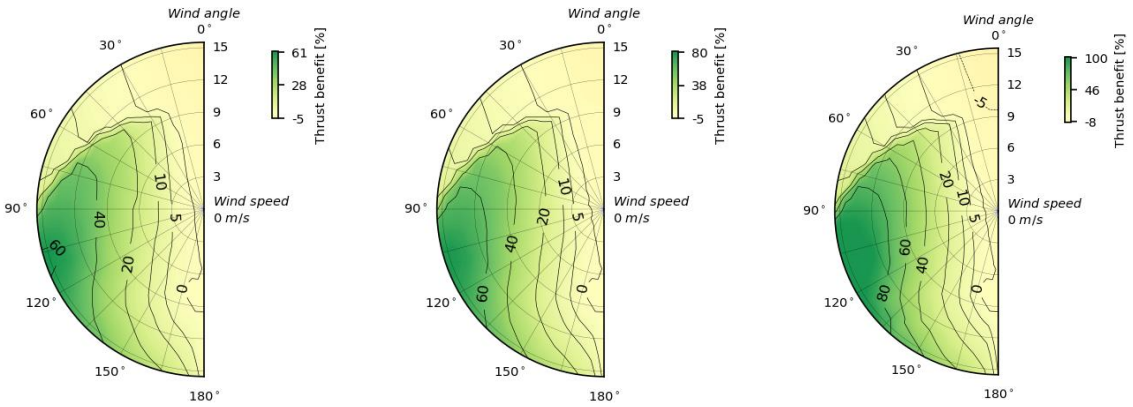


Fig.10: Polar diagram showing thrust benefit in terms of True Wind condition for design candidates three wingsails (left), four wingsails (center), and six wingsails (right). (Vs = 18 kn)

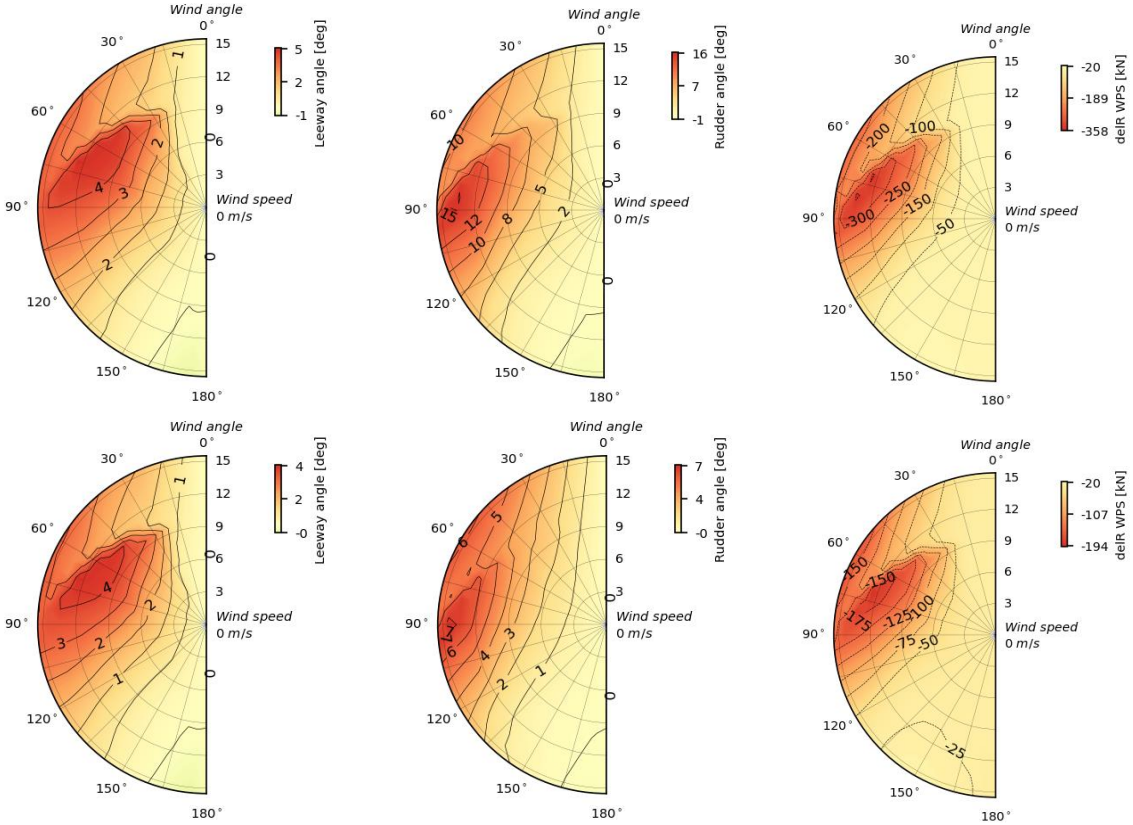


Fig.11: Leeway and rudder angle presented as polar diagram for True Wind condition. Bare hull (top) and Anti-drift fin case (bottom). Six wingsails, Vs=18 kn.

Vessel response polar diagrams of heel (using GM =3.5 m), leeway, and rudder angle show no major blocking issues. HUMBRIA SEAWAYS operates at high transit speeds, with ample flow over dual rudders providing steady course-keeping even under wind propulsion drift force. Anti-drift fins are incorporated in the design to improve upwind efficiency and cope with generally small apparent wind angles associated with high transit speeds, following *Jacobi et al. (2024)*. The impact is presented in Fig.11 showing polar diagrams for leeway and rudder angles for the six wingsails configuration.

3.3.3. Operational Profiles and Voyage Simulations

Wind data for the route between Gothenburg and Ghent, expressed as percentiles in a wind scatter matrix, are used to create a weighted sum of the entries in the polar diagram, giving the expected performance of the design candidate sailing along the route.

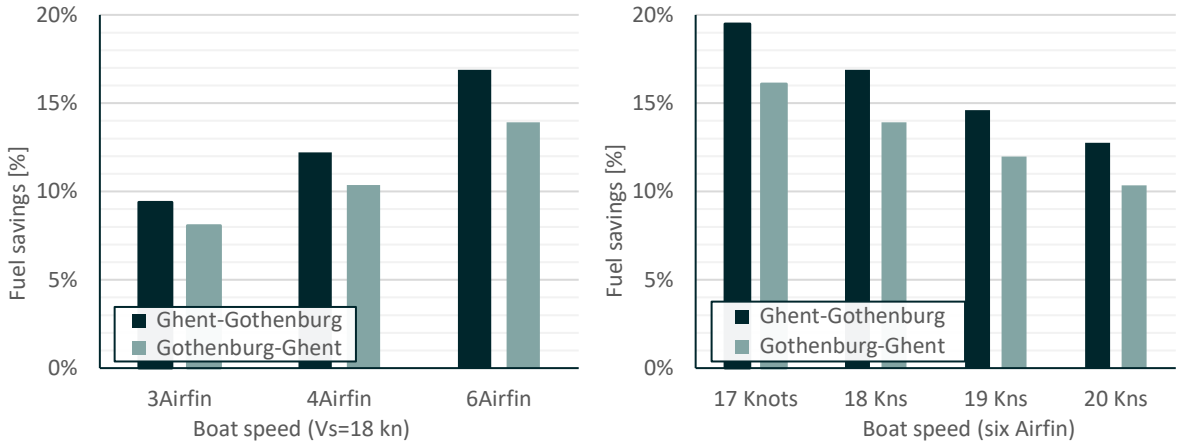


Fig.12: Percentage of fuel saved per voyage calculated using annual wind statistics showing performance of different sail configurations (left) at vessel speed 18 kn, and impact of vessel speed (right) for six Airfin configuration as maximal retrofit option.

We obtain a rough indication (with fixed speed) of expected voyage fuel savings of approximately 10 ton per voyage, corresponding to between 8% and 19% according to number of wingsails or vessel speed, shown in Fig.12.

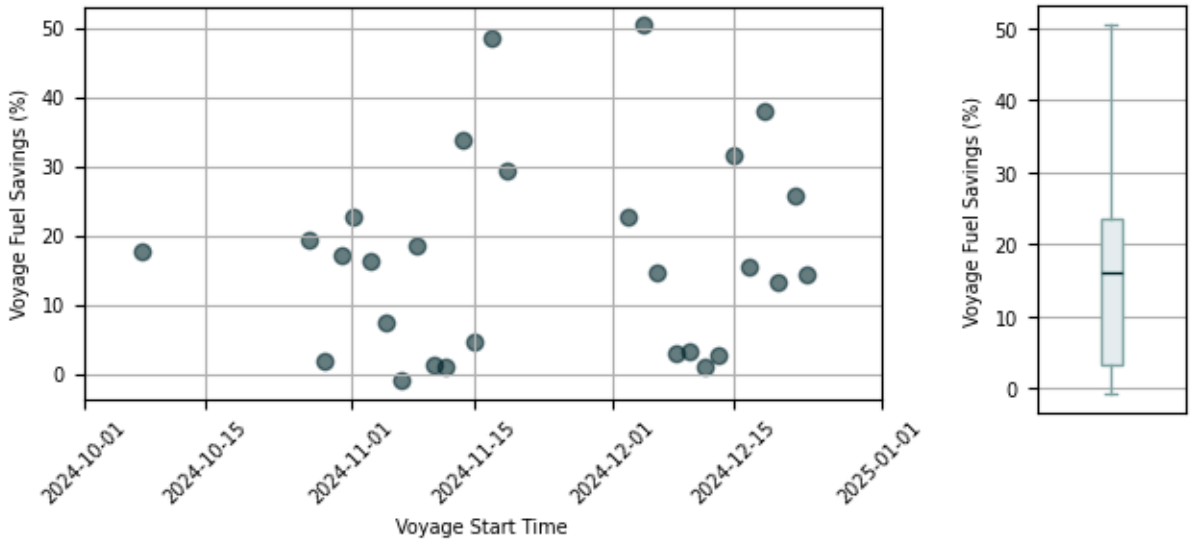


Fig.13: Tons of fuel saved per voyage calculated as 28 individual realizations based on AIS voyage tracks of during Q4 2024

Wind propulsion contribution on individual voyages was computed by comparing consumption of the Airfin arrangements with the baseline ship model along voyage AIS tracks. Each result is shown in Fig.13, including resulting statistics for the voyage fuel savings. The median value for individual realisations presented is 16%, with interquartile range of 3.3%-23.6%. In ongoing work, this analysis will be extended to consider seasonal and interannual variation in wind conditions.

4. Discussion & Conclusions

This study demonstrates the technical feasibility and substantial operational benefits of retrofitting high-speed RoRo vessels with rigid wingsail systems. Through advanced aerodynamic modelling, CFD-informed interaction analysis, and validated operational simulations, we find that significant thrust contribution from wind propulsion is achievable even at service speeds around 17–19 kn. The case study of HUMBRIA SEAWAYS shows potential fuel savings of up to 50% on individual

voyages, with a median reduction of 16% over a winter sailing season. Key to unlocking this performance is the aerodynamic efficiency of modern wingsails, especially in upwind conditions where apparent wind angles are small. Integration considerations, such as anti-drift fins and deck layout, also play a vital role in maximising benefit while maintaining vessel operability. This research strengthens the business and technical case for wind-assist retrofits in high-speed RoRo fleets operating along windy, regular trade routes.

Acknowledgments

We thank DFDS for transparently sharing design and operational data in support of this research. We also thank Clément Gouriou at CWS for his kind help with the CFD simulations of the ship.

References

BHAGWAT, M.; LEISHMAN, G. (2002), *Generalised viscous vortex model for application to freevortex wake and aeroacoustic calculations*, 58th American Helicopter Society Annual Forum, Montreal

BORDOGNA, G.; KEUNING, L.; HUIJSMANS, R.; FOSSATI, F.V.; BELLOLI, M. (2016), *Validation of a simple aerodynamic model capable to predict the interaction effects occurring between two generic wind propulsion systems*, 12th Int. Conf. on Hydrodynamics (ICHD), Egmond aan Zee

CLAUGHTON, A.; PEMBERTON, R. (2012), *Hull–Sailplan Balance, "Lead" for the 21st Century*, 22nd Int. HISWA Symp. Yacht Design & Yacht Construction, Amsterdam

DNV (2023), *Always on schedule with rotor sails: a captain tells his story*, https://www.dnv.com/expert-story/maritime-impact/Always-on-schedule-with-rotor-sails-a-captain-tells-his-story/

GARENAUX, M.; SCHOT, J. (2021), *Flettner rotors performance and interaction effects on the MARIN hybrid transition coaster*, Wind Propulsion Conf., London

MALMEK, K.; DHOME, U.; LARSSON, L.; WERNER, S.; RINGSBERG, J.; FINNSGÅRD, C. (2020), *Comparison of two rapid numerical methods for predicting the performance of multiple rigid wing-sails*, 5th Int. Conf. Innovation in High Performance Sailing Yachts and Sail-Assisted Ship Propulsion

MALMEK, K.; LARSSON, L.; WERNER, S.; RINGSBERG, J.; BENSOW, R.; FINNSGÅRD, C. (2024), *Rapid aerodynamic method for predicting the performance of interacting wing sails*, Ocean Eng. 293

MASON, J.; LARKIN, A.; BULLOCK, S.; VAN DER KOLK, N.J.; BRODERICK, J.F. (2023), *Quantifying voyage optimisation with wind propulsion for short-term CO_2 mitigation in shipping*, Ocean Eng. 289/1

MINAMI, Y.; NIMURA, T.; FUJIWARA, T.; UENO, M. (2003), *Investigation into Underwater Fin Arrangement Effect on Steady Sailing Characteristics of a Sail Assisted Ship*, 13th ISOPE Conf., Honolulu

TARDIF, T.; GOURIOU, C.; STELLA, F. (2024), *Enhancing confidence in multi-sail performance prediction: a comparative study of aerodynamic interactions models with wind tunnel data*, Wind Propulsion Conf., London

VAN DER KOLK, N.J. (2020). *Sailing efficiency and course keeping ability of wind-assisted ships*, PhD thesis, Delft University of Technology

VAN DER KOLK, N.J.; AKKERMAN, I.; KEUNING, J.A.; HUIJSMANS, R.H.M. (2021), *Low-aspect ratio appendages for wind-assisted ships*, J. Marine Science and Technology 26, pp.1126-1143